

Original Article

Optimization of Operating Factors and Blending Levels of Diesel, Algae Methyl Ester, Graphene Oxide and Producer Gases - Calorific Values Using Response Surface Methodology in HCCI Engine

M. Prabhakar^{1*}, S. Prakash², S. Nallusamy², S. Ponnarasu¹, Yeddula Deekeshwar Reddy¹

¹Department of Mechanical Engineering, Aarupadai Veedu Institute of Technology, Vinayaka Mission's Research Foundation, Deemed to be University, Tamil Nadu, India.

²Department of Adult, Continuing Education and Extension, Jadavpur University, Kolkata, India.

*Corresponding Author: mprabhakar@gmail.com

Received: 14 October 2023

Revised: 19 November 2023

Accepted: 10 December 2023

Published: 20 January 2024

Abstract - An experimental investigation was conducted in this study to assess the effects of adding different levels of Graphene Oxide (GO) 25, 50, and 75 ppm on engine parameters in an HCCI engine operating with a blend of 20, 40, and 60% Algae Methyl Ester (AME). The quality of PG is critical for running power generation engines at the desired performance level. A mathematical analysis was performed on a Homogeneous-Charge Compression Ignition (HCCI) diesel engine for CV of PG from 10, 20, and 30 MJ/Nm³ of coconut shell, which was included in this study. Following that, an optimization using Response Surface Methodology (RSM) was performed to establish the optimal working conditions at various engine loads. According to the results of the experiments, GO additives are an excellent addition to diesel-AME blends to improve performance as well as decrease emissions. The model predicted the best result with predicted and actual graphs, with the lower BTE being 20.25%. The higher BTE is 26%, the lower BSFC is 1.69 kg/kWh, the higher BSFC is 2.46 kg/kWh, and the lower CO content of the exhaust is 0.04 vol%. The higher CO content is 0.22 vol%, the lower HC emission is 18.82 ppm, the higher HC emission is 30.3 ppm, and the lower NoX emission is 201 ppm. In contrast, the more significant NoX emission is 301 ppm; lower smoke emissions are reported at 21.01%, whereas higher smoke emissions are reported at 35.4%. According to the study's findings, it is possible to conclude that the RSM model may effectively model an HCCI diesel engine, saving time and money.

Keywords - Diesel engine, HCCI, Algae Methyl Ester, Emission, Optimization.

1. Introduction

Rising greenhouse gas emissions from burning more fossil fuels are a significant contributor to air pollution and global warming. It is projected that 3 million deaths occur each year due to air pollution created by vehicles powered by fossil fuels in manufacturing, power generation, and transport, and this quantity is expected to rise to 5.5 million by 2050 [1]. It is generally accepted that switching to renewable energy sources is the best way to decrease or eliminate harmful air emissions from the combustion of fossil fuels [2]. Improved fuel composition and manufacturing/after-treatment engine techniques are both necessary for reducing vehicle emissions. Biomass is an alternative form of energy that has advantages for the environment and economic growth, and it has the potential to do both [3]. The thermochemical approach has been shown to be both environmentally friendly and commercially successful in a number of investigations. The qualities of biodiesel are strongly influenced by the form of

material that is used in its production and the techniques employed during that manufacture [4]. Researchers have a higher opinion of biodiesels made from vegetable oils. Because Rudolph Diesel's first diesel engine was able to run on vegetable oil, it follows that biodiesel made from plants is an excellent replacement fuel for diesel vehicles [5]. Biodiesel can be made from a variety of vegetable oils. However, this one stands out as a viable biodiesel raw material due to its capability to enhance cold flow qualities while maintaining the stability of oxidation [6]. Emissions, fuel supply and transportation, and the impact on engine durability are all crucial considerations when evaluating alternative fuels for usage in diesel engines [7]. Recent researchers have observed that fuel composition techniques offer the most significant potential for enhancing engines' broad range of attributes [8]. A technique employing microparticles, which will produce aggregating issues within the fuel, nanoparticles are capable of being used to achieve a homogeneous distribution



throughout the fuel. Studying the effects of adding an additive to biodiesel blends, researchers found that the fuel's BTE could be enhanced thanks to better mixing and more surface area for the fuel/oxygen response, as well as higher combustion and evaporation of the fuel's particles [9]. Biodiesel blends often included Dimethyl Ether (DME) as an addition because of its high oxygen concentration, which enhanced the combustion reaction and boosted BTE [10].

One exciting innovation is the use of non-metallic GO combined with fuel to boost engine performance and reduce pollution. Combined GO additives and tested their impact on emission qualities in diesel engines by adding them at varying concentrations to fuel blends comprising fish oil methyl ester [11]. The tests were conducted at a steady velocity and with varying engine loads. According to the authors, GO additive improves combustion quality by raising the oxygen-to-fuel ratio in the cylinder [12]. The reason, they indicated, is that NoX emissions were reduced by 12.5% and CO emissions by 28.23%. Furthermore, it was reported that the enhanced thermal characteristics of the GO additive led to an 18.27% decrease in HC emission [13]. According to the authors, when GO additive was included in the test fuels, the energy content increased, leading to a 17.80% increase in BTE and a 10.82% decrease in BSFC. In addition, the thermo-chemical transformation approach was proposed as a viable green replacement for traditional power plants.

Waste materials such as garbage shells [14], rubber shells [15], coconut shells [16], and so on that are readily available in rural areas have been the focus of experimental investigations in prior studies. Producer Gas (PG) with a heating value of 5–8 MJ/Nm³ was seen to be created. Extensive discussion of the consequences of biomass moisture, the optimal equivalency ratio, gas output, and gasifier performance may be found in the previously mentioned sources [17]. Engineering challenges can be analysed by modelling and optimising the RSM that is affected by experiment factors, which is where Response Surface Methodology (RSM) [18]. This multidimensional statistical approach effectively optimises the effects of many parameters and the interactions between the variables to obtain the best system function [19].

The primary benefit of RSM-based experimentation design is its reduced testing and time requirements in comparison to complete factorial experimentation [20]. As stated in the literature cited above, the most effective Algae Methyl Ester (AME)/diesel fuel combination is found in limited research tests has been done. The goal is to find the best volume of GO with the fewest number of experiments possible by optimising with RSM. In CI engines, PG from different feedstocks is used along with diesel and biodiesel. Also, the CV of PG is not the same for all the feedstock that can be found in remote regions. It is important to study how engines work in all operating conditions and how the CV of

PV changes at different load conditions in order to make better use of biofuel for more uses. The main goal of the investigation was to find out what happens when the CV of PG changes in a gas-diesel engine that uses different types of Coconut Shells (CS). Response Surface technique and the right tools were used to make the model.

2. Materials and Methods

Due to their readily accessible and non-toxic characteristics, algae have been recognized as a prospective biodiesel source [21]. Aqueous and coastal waters are the residence of these photosynthetic algae, whose productivity can be multiplied in a shorter period when grown under controlled circumstances [22].

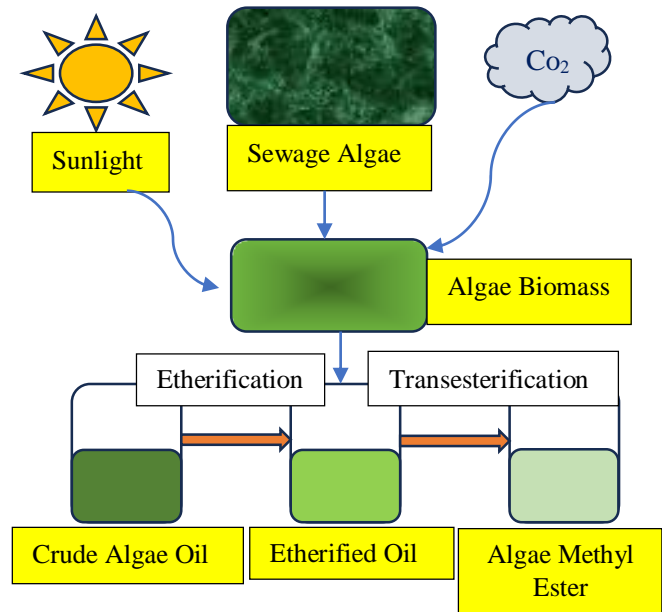


Fig. 1 Preparation of Algae Methyl Ester

Table 1. Chemical properties of diesel, Algae oil Methyl Ester and methanol

Properties	ASTM Standard	AOME
Density (kg/m ³)	D127	895
Kinematic Viscosity @ 40°C (cSt)	D2217	4.07
Calorific Value (MJ/kg)	D4809	39
Flash Point (°C)	D93	107
Fire Point (°C)	D93	120
Cetane Number	D6890	52.6
Oxygen (%) by wt	D943	-

As dietary supplements, these algae are utilized in numerous nations. Due to its potent odour, frequent usage is discouraged. Pharmaceutical applications are also feasible as a result of their therapeutic attributes. It is an excellent biofuel source, and the Algae Methyl Ester (AME) it generates is being evaluated as a possible fossil fuel replacement. Algal might be utilized as an alternative fuel to extract methyl ester due to its high level of lipids. These algal organisms produce methyl esters of 14–18 carbon fats using a considerable quantity of oxygen.

The AME preparation is illustrated in Figure 1. The chemical properties of AME are presented in Table 1. However, waste biomass such as coconut shells that are thrown away are not successfully applied and are instead burned in the open air [23]. Coconuts make up the majority of agricultural production; however, this waste biomass is not appropriately utilized [24]. If the right technology is applied, each of the types of biomass that have been discussed above possesses the capability of being transformed into forms that can be utilized in the generation of beneficial forms of energy. In addition, the energy that is taken from these types of biomass can be utilized to power internal combustion engines, which are then used to generate electricity.

As a consequence of this, the biomasses that were discussed earlier underwent testing in a gasifier that is part of this research and can be purchased. Because variations in the CV of producer gas affect the operating characteristics of HCCI engines, it was necessary to examine the typical gas composition and CV of PG derived from the various materials.

3. Experimental Setup and Procedure

An investigation has been carried out for the purpose of determining the impact of adding various levels of Graphene Oxide (GO) with the range of 25 ppm, 50 ppm, and 75 ppm on the engine parameters of an HCCI engine that was working with an additive fuel mixture. GO is a unique chemical element. GO has an additive function as a single atomic layer of carbon that has been functionalized.

Due to the presence of this additive particle duality, GO is an exciting substance to investigate from the point perspective of both chemistry and materials science. In addition, the fuel combination of AME and GO additive that is used in HCCI engines and observed data is optimized. An internally compressed, four-stroke, single-cylinder gasoline engine with port injection was transformed into an HCCI engine.

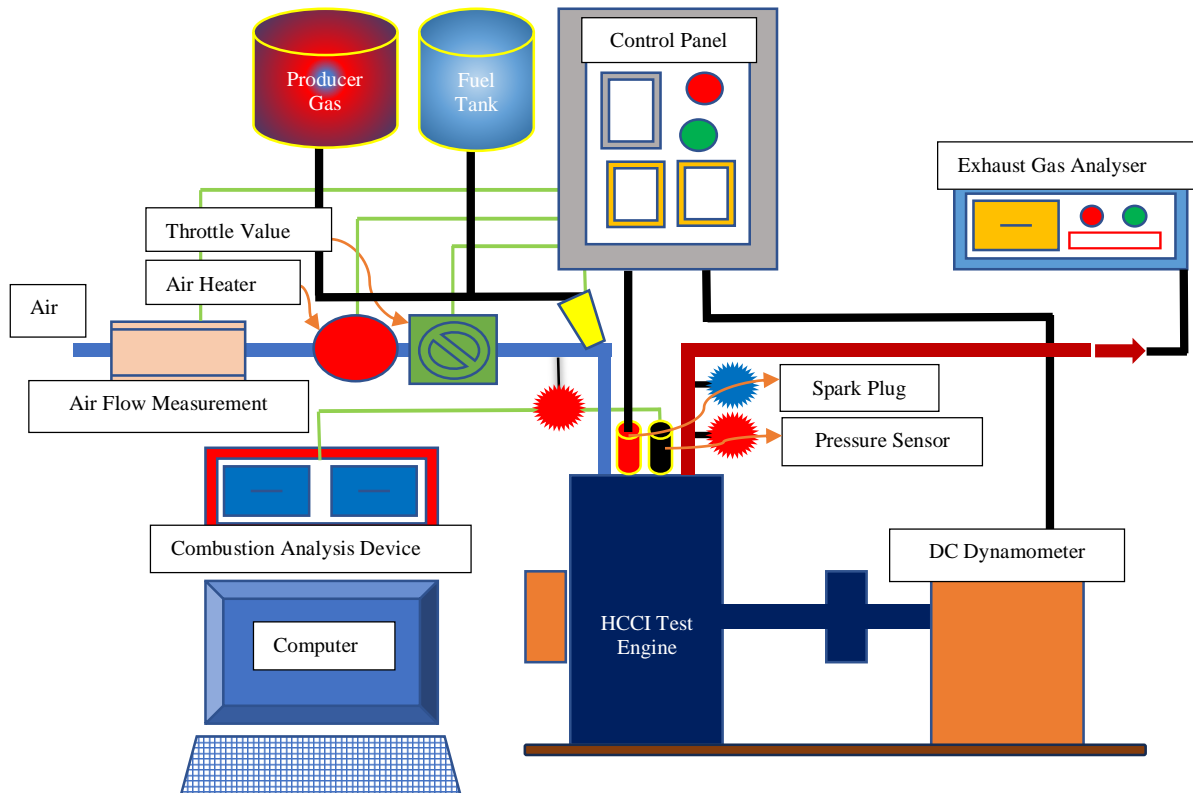


Fig. 2 Experimental setup

The intake and exhaust valve elevations for the gasoline engine are both 9 mm at the factory. For intake and exhaust cams, valve elevations were decreased to 3 mm and 5 mm, accordingly, so as to achieve HCCI operation. To achieve this objective, a novel camshaft was devised and integrated into the engine, which allows for the adjustment of cam angles along the shaft [25]. A DC dynamometer with a power rating of 6500 revolutions per minute was employed to apply strain to the test engine. The engine speed was determined using a pickup sensor on the dynamometer controlling unit. The pressure within the piston was assessed by means of a piezoelectric transducer. Furthermore, in order to ascertain the Top Dead Centre (TDC) and measure engine speed, an encoder was affixed to the crankshaft.

A data acquisition device was utilized to transform analogue cylinder pressure data into digital format. Additionally, the fuel ratio was adjusted using the potentiometer located on the dynamometer controlling box. Alterations were made to the configuration in order to utilize the engine in biofuel mode subsequent to the conclusion of all foundational investigations utilizing diesel. A gas regulator controlled the flow rate of PG, which was subsequently combined with the incoming air. By passing diesel through an intake manifold at 23° BTDC under 230 bars of pressure, the air-PG mixture was nourished. Figure 2 presents a schematic representation of the experimental configuration.

3.1. Construction of RSM

This study’s experimental design makes use of four independent variables in order to separate the effects of the operational parameters, quadratic factors load, AME blend, CV of PG, and Graphene Oxide in Table 2. Model-fitting designs require a minimum of three levels per variable. Box-Behnken in design expert software satisfies this need with its three categories for each variable.

By incorporating two investigational ideas, each coordinate axis on reverse sides of the starting point and at a distance equivalent to the semi-parallel of the cubic of the factorial design, as well as new extreme outcomes (low and high) for every variable included in this design, the box - Behnken design becomes the most effective and best of all designs. A Box-Behnken technique using design expert software was applied for the present investigation to gather the results of the experiment, which would correspond to complete second-order polynomial models describing the RSM across a comparatively wide variation of parameters.

The studies were carried out in accordance with the experiments that were designed, and all of the essential parameters, including load, AME blend, CV of PG, and Graphene Oxide, were monitored. The response variables were computed using standard relations based on the data from the experiments, and the results are presented in Table 3.

Table 2. Construction of RSM process parameters

Process Parameters	Levels		
	1	2	3
A - Load (KG)	1.3	2.6	3.9
B - AME Blend (%)	20	40	60
C - CV of PG - (MJ/Nm3)	10	20	30
D - Graphene Oxide (ppm)	25	50	75

4. Result and Discussion

The performance parameters of the AME CV of PG and GO operated in an HCCI engine, such as performance and emission, were enhanced with the design variables. The regression coefficient, typically referred to as R2, is a measurement that can be used to estimate how accurately the model can predict reactions based on actual experimental results. R2 is an abbreviation for the regression coefficient. An indicator known as R2 reflects the prediction of independent variables, and its value can range from 0 to 1 at any one time.

In the situation when R2, the model’s capability to forecast results is shown to be more accurate. It is feasible to attain a higher adjusted R2 by minimizing the number of features that are regarded unimportant as a part of the adjustment process. This section analyzes the variance of R2 with respect to each of the replies. It is possible to conclude from these findings that the experiments have a high degree of precision. The average P-value for BTE is 0.53, the average P-value for BSFC is 0.41, the average P-value for CO is 0.44, the average P-value for HC is 0.64, and the average P-value for smoke is 0.63. Given that this is the case, it may be deduced that BP is a more critical factor than CV in regard to all of the responses.

4.1. BTE – AME Blends, CV of PG and GO

According to the observed factors, the obtained quadratic model of BTE as suited using RSM related in Equation (1),

$$\begin{aligned}
 \text{(BTE)} = & 31.9824 + -2.12821 * A + 0.0104583 * \\
 & B + -0.219917 * C + -0.124333 * D + \\
 & -0.0341346 * AB + 0.13 * AC + 0.0205385 * AD + \\
 & -0.0019625 * BC + 0.002245 * BD + -0.00168 * \\
 & CD) \tag{1}
 \end{aligned}$$

The effect of the quadratic factors load, AME blend, CV of PG and Graphene Oxide was initiated to be very important (P =0.76) on the performance of BTE. All fair terms were determined to be significant, indicating a curving connection between the experiment’s factors and BTE performance. According to the 3D surface plots in Figure 3(a) relating to the load vs AME blend, the increase in BTE while increasing the

load and AME blend is caused by the lower viscosity and increased calorific value. The 3D surface plots connected to the impact of PG-CV Figure 3(b) and BP on BTE performance when the load decreases the CV towards the PG increases, BTE increases with a rise in BP with a rise in CV may be attributable to high burns rate as well as rapid combustion progress. When a low CV of PG is delivered into the combustion area, it lowers the entering of new air, resulting in incomplete combustion and low BTE. The 3D surface plots in

Figure 3(c) of load vs. Graphene Oxide both enhanced the quantity of GO and had a beneficial influence on BTE. After raising the GO, however, the BTE value began to exhibit a downward trend. The influence of engine load on BTE was more apparent when compared to the change in GO quantity. Because the result falls within this range, the accuracy of the suggested optimization is proven using the predicted and actual graphs shown in Figure 3(d), where the lower BTE is 20.25% and the higher BTE is 26%.

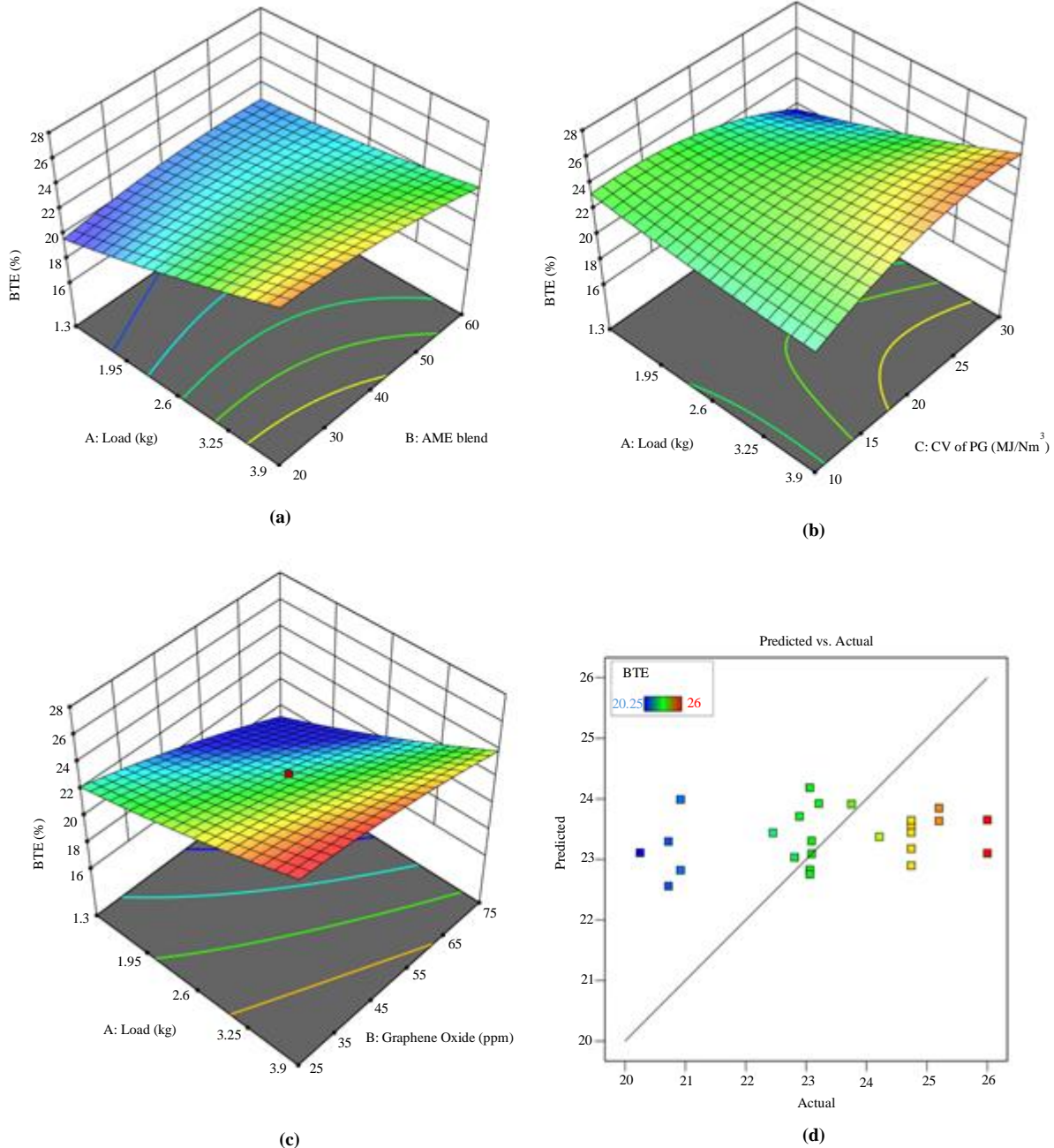


Fig. 3 BTE (a) Load vs. AME, (b) Load vs. CV of PG, (c) Load vs. Go, and (d) Predicated vs. Actual.

4.2. BSFC – AME Blends, CV of PG and GO

According to the observed factors, the obtained quadratic model of BSFC as suited using RSM related in Equation (2),

$$(BSFC = 1.7244 + 0.133974 * A + -0.00995833 * B + -0.001 * C + 0.016 * D + 0.00663462 * AB + -0.0103846 * AC + -0.00476923 * AD + 0.000225 * BC + -0.0003 * BD + 0.00044 * CD)(2)$$

The effect of the quadratic factors load, AME blend, CV of PG and Graphene Oxide was found to be lower significant (P=0.55) on the fuel consumption of BSFC. All square terms were likewise determined to be significant, implying a curving

connection between the experiment’s variables and BSFC fuel usage. The 3D surface graphs shown in Figure 4(a) relating to the load vs AME mix show that the BSFC decreases with increasing power for both biofuels due to an increase in combustion chamber temperature. The increased BSFC of biodiesel blends may be attributable to the decreased calorific value of that fuel, especially compared with diesel. The 3D surface plots in Figure 4(b) relate to the impact of PG- CV and BP on BSFC consumption of fuel; whenever PG with low CV is utilized, it slows the rate of combustion due to the low density of energy of PG, which stimulates the availability of more diesel and produces a decrease in BSFC fuel consumption.

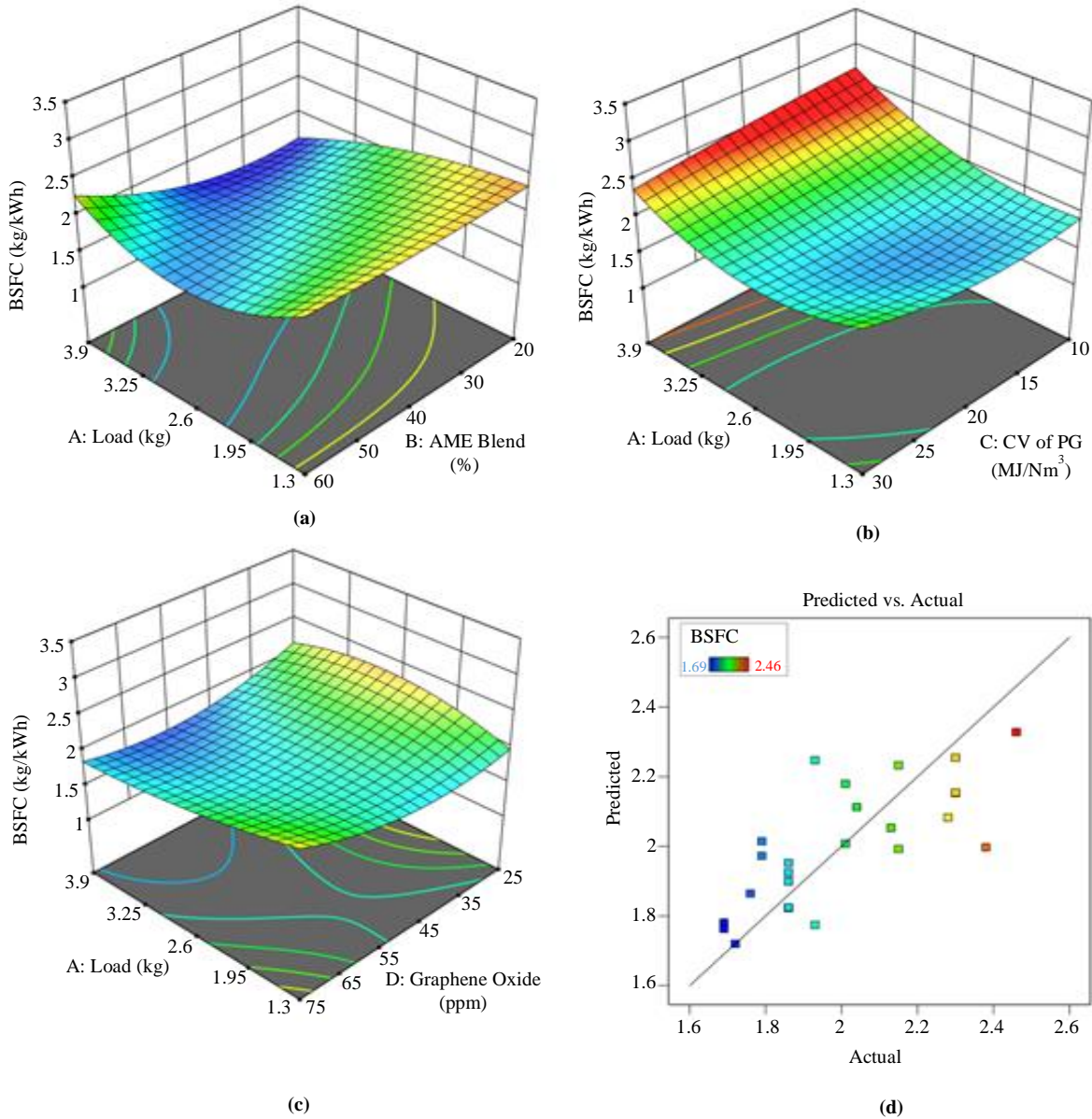


Fig. 4 BSFC (a) Load vs. AME, (b) Load vs. CV of PG, (c) Load vs. Go, and (d) Predictated vs. Actual.

The decrease in BSFC with increasing BP could be attributed to the improved combustion characteristics of the PG/diesel mixture. Furthermore, greater combustion value and resultant decreases in fuel consumption happen due to the increased fuel reactivity provided by the GO additive shown in Figure 4(c).

Finally, it can be shown that a more significant engine load has a favourable effect on the BSFC. At heavy loads, the BSFC drops as thermal efficiency increases. Because the outcome falls within this range, the suggested optimization's correctness is proven by the predicted and actual graphs shown in Figure 4(d). The lower BSFC measured is 1.69 kg/kWh, and the higher BSFC measured is 2.46 kg/kWh.

4.3. CO – AME Blends, CV of PG and GO

According to the observed factors, the obtained quadratic model of CO emission as suited using RSM related in Equation (3),

$$\begin{aligned} \text{CO} = & 0.308667 + -0.0288462 * A + \\ & 0.000458333 * B + -0.00975 * C + -0.0025 * D + \\ & -0.00144231 * AB + 0.00384615 * AC + \\ & 0.000461538 * AD + 2.5e - 05 * BC + 5e - 05 * \\ & BD + -5e - 05 * CD \end{aligned} \quad (3)$$

The effect of the quadratic factors load, AME blend, CV of PG and Graphene Oxide was found to be lower significant (P =0.60) on the exhausts CO emission.

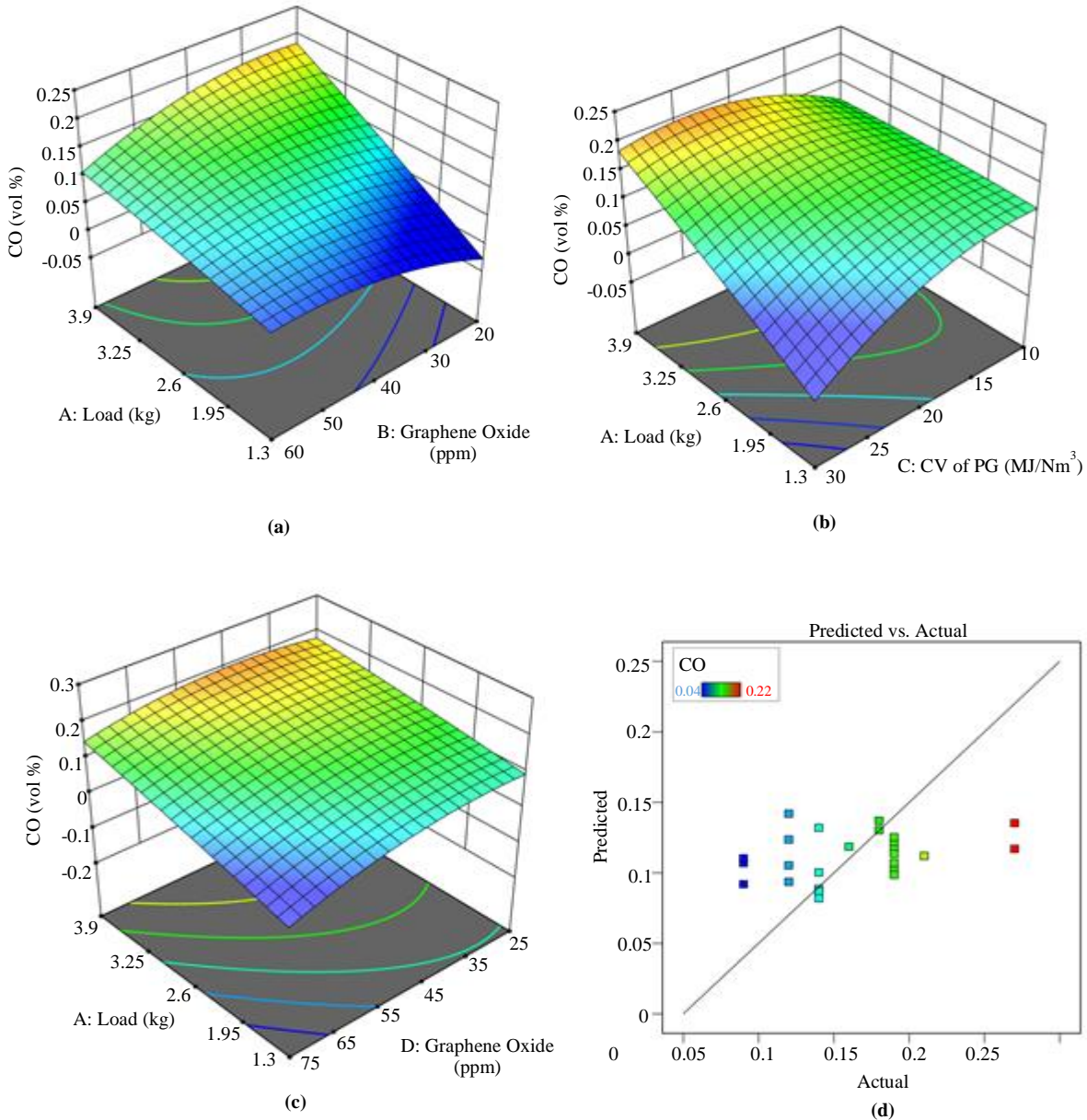


Fig. 5 CO (a) Load vs. AME, (b) Load vs. CV of PG, (c) Load vs. Go, and (d) Predicted vs. Actual.

All square terms were likewise found to be significant, indicating a curving connection between the experiment's variables and CO emission from the exhaust. The 3D surface graphs are shown in Figure 5(a) relating to load vs AME mix show that the AME blend results in lower CO emissions than diesel at the highest level of output. The excessive amount of O² molecules in biodiesel, which increases the process of oxidation and hence reduces CO emissions, maybe the cause of the drop in CO emissions for AME blends.

The 3D surface plots shown in Figure 5(b) relate to the impact of PG-CV and BP on the formation of exhaust CO emission drop with a reduction in both CV and BP as load increases, and it achieves the optimal value.

When BP and CV are raised, the most minor CO is obtained. Because of the low CO emission under this circumstance, the fuel will probably burn effectively in comparison to all other circumstances. The 3D surface plots shown in Figure 5(c) relate to the load vs Graphene Oxide. The surface graph illustrates the change in CO emission, which constitutes one of the hazardous pollutants produced by partial combustion, relying on the GO towards the load.

Despite the reduction in CO emission caused by the four adding GO being almost negligible, a modest decrease is being observed. The vast surface area of GO increases load and reduces the ignition delay, improving combustion. CO emissions decrease as combustion improves.

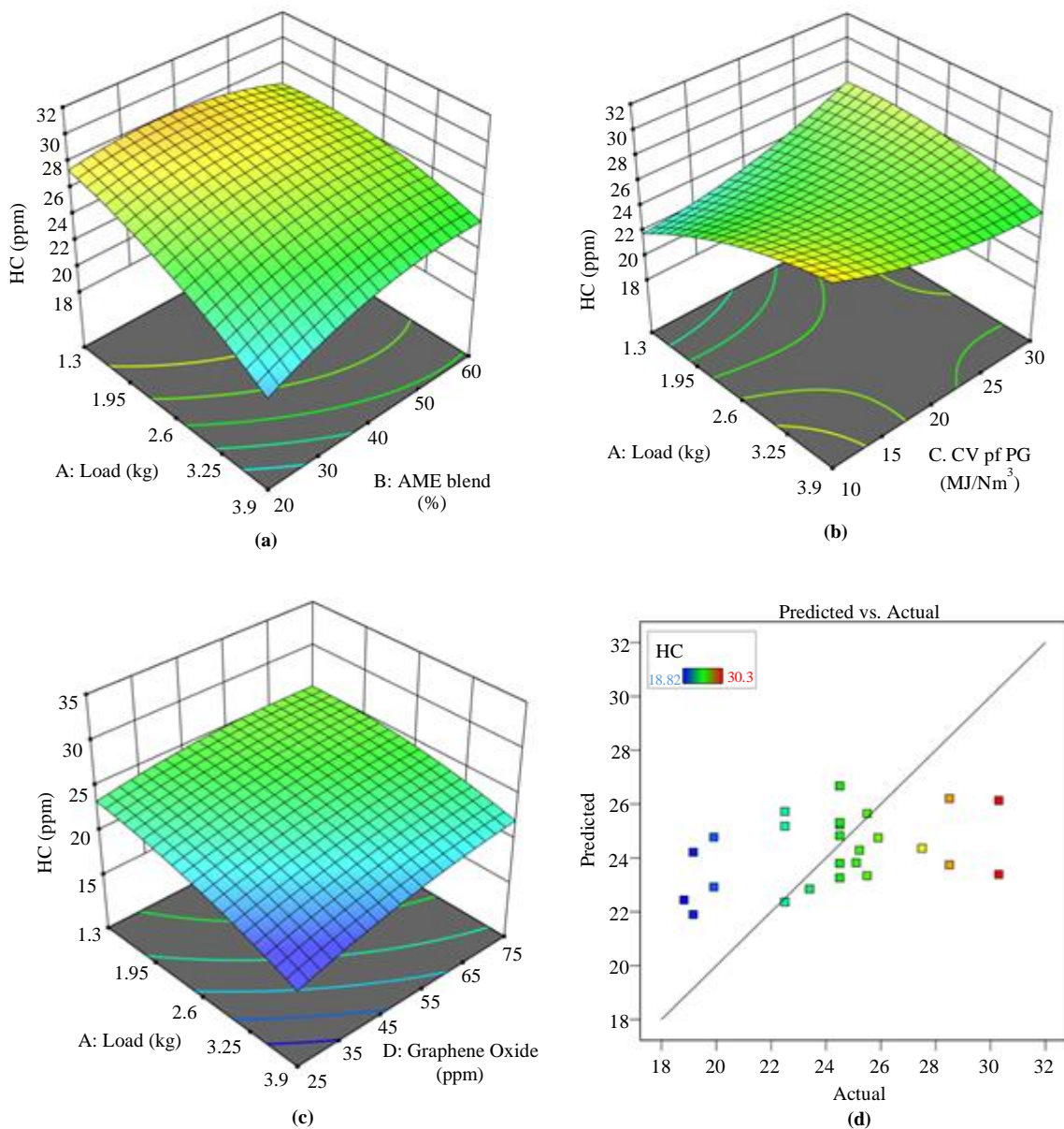


Fig. 6 HC (a) Load vs. AME, (b) Load vs. CV of PG, (c) Load vs. Go, and (d) Predicted vs. Actual.

Because the outcome falls within this range, the proposed optimization's correctness is proven by the predicated and actual graphs shown in Figure 5(d); the lower CO content of the exhaust is 0.04 vol%, while the higher CO content is 0.22 vol%.

4.4. HC – AME Blends, CV of PG and GO

According to the observed factors, the obtained quadratic model of HC emission as suited using RSM related in Equation (4).

$$(HC = 10.9639 + 0.110256 * A + 0.0650417 * B + 0.682583 * C + 0.0872667 * D + 0.0441346 * AB + -0.161346 * AC + 0.0238462 * AD + -0.00235 * BC + -0.0015 * BD + -0.002 * CD) \quad (4)$$

The effect of the quadratic factors load, AME blend, CV of PG and Graphene Oxide was found to be lower significant (P=0.34) on the exhausts HC emission. All square terms were likewise found to be significant, indicating a curving connection between the experiment's variables and the HC emission of the exhaust. According to the 3D surface plots shown in Figure 6(a) relating to the load vs AME mix, AME blend results in decreased HC emissions, which are created primarily due to the abundance of gaseous hydrocarbons in the relatively stationary low-temperature boundary layer that lies along the cylinder wall and within the services. Because the flame fails to extend into these zones completely, hydrocarbon stays unburned. The 3D surface plots shown in Figure 6(b) pertain to the influence of PG- CV and BP on the creation of exhaust HC emissions; the primary cause of this emission is incomplete fuel combustion.

The insufficient combustion of AME fuel could be the cause. When CV is lowered, the emission of HC for all BPs continues to increase. The 3D surface plots shown in Figure 6(c) that relate to the load vs Graphene Oxide the surface graph depicting the change of HC emission, it can be recognized that the HC emission reduces quickly with the rise in the GO quantity but increases rapidly with increasing engine load. Because there is inadequate time for homogenous mix production at high loads, the portion of the fuel will not meet with oxygen, and HC is projected to rise as the load rises. The fundamental explanation for the decrease in HC emissions caused by the introduction of GO is that GO promotes combustion by boosting chemical reactions and decreasing ignition latency. Because the outcome falls within this range, the proposed optimization's correctness is proven by the predicated and actual graphs shown in Figure 6(d). The lower HC emission is 18.82 ppm, whereas the higher HC emission is 30.3 ppm.

4.5. NoX – AME Blends, CV of PG and GO

According to the observed factors, the obtained quadratic model of NoX emission as suited using RSM related in Equation (5),

$$(NoX = 288.253 + -21.7308 * A + 1.48333 * B + -0.525 * C + -1.75333 * D + -0.875 * AB + 1.73077 * AC + 0.569231 * AD + -0.035 * BC + 0.0345 * BD + -0.055 * CD) \quad (5)$$

The effect of the quadratic factors load, AME blend, CV of PG and Graphene Oxide was found to be lower significant (P =0.61) on the exhausts NoX emission. All square terms were likewise found to be significant, indicating a curving connection between the experiment's variables and NoX emission from the exhaust. According to the 3D surface plots shown in Figure 7(a) relating to the load vs AME blend, NoX emissions are created chiefly from nitrogen present in the ambient air entering the engine due to excessive combustion temperature throughout the process of combustion. The 3D surface plots shown in Figure 7(b) relating to the impact of PG-CV and BP on the creation of exhaust NoX emission show that the calculated NoX is near to the experimental measurements, demonstrating the model's dependability. The more significant inflow of low-CV PG into the burning chamber lowers its temperature, which may minimize NoX emissions.

In contrast, a high CV-producing gas increases NoX emissions. The 3D surface plots shown in Figure 7(c) relating to load vs Graphene Oxide, the surface graph displaying the change of NoX emission, it is evident that the addition of GO impacts NoX emission favourably and engine load negatively. Temperature, local oxygen content, and combustion time all have an impact on NoX generation. There are actually two main approaches for lowering NoX emissions: lowering the flame temperature and lowering the introduction of GO promotes a shorter combustion duration. NoX emissions, on the reverse together, increased as the engine load raised in-cylinder temperature. Because the outcome falls within this range, the proposed optimization's correctness is proven by the predicated and actual graphs shown in Figure 7(d). The lower NoX emission is 201 ppm, whereas the more significant NoX emission is 301 ppm.

4.6. Smoke – AME Blends, CV of PG and GO

According to the observed factors, the obtained quadratic model of smoke emission as suited using RSM related in Equation (6),

$$(Smoke = 14.7019 + 0.808974 * A + 0.253667 * B + 0.412833 * C + -0.0344667 * D + -0.0645192 * AB + 0.00596154 * AC + 0.0507692 * AD + -0.0031125 * BC + 0.00065 * BD + -0.0046 * CD) \quad (6)$$

The effect of the quadratic factors load, AME blend, CV of PG and Graphene Oxide was found to be lower significant (P=0.38) on the exhaust smoke emission. All square terms were determined to be significant, indicating a curving

connection between the experiment's variables and exhaust smoke emission. The 3D surface plots shown in Figure 8(a) relating to the load vs AME blend show that smoke opacity

decreases for biodiesel blends due to increased oxygen present in it, which accelerates the oxidation process of the fuel mixes, resulting in less smoke opacity.

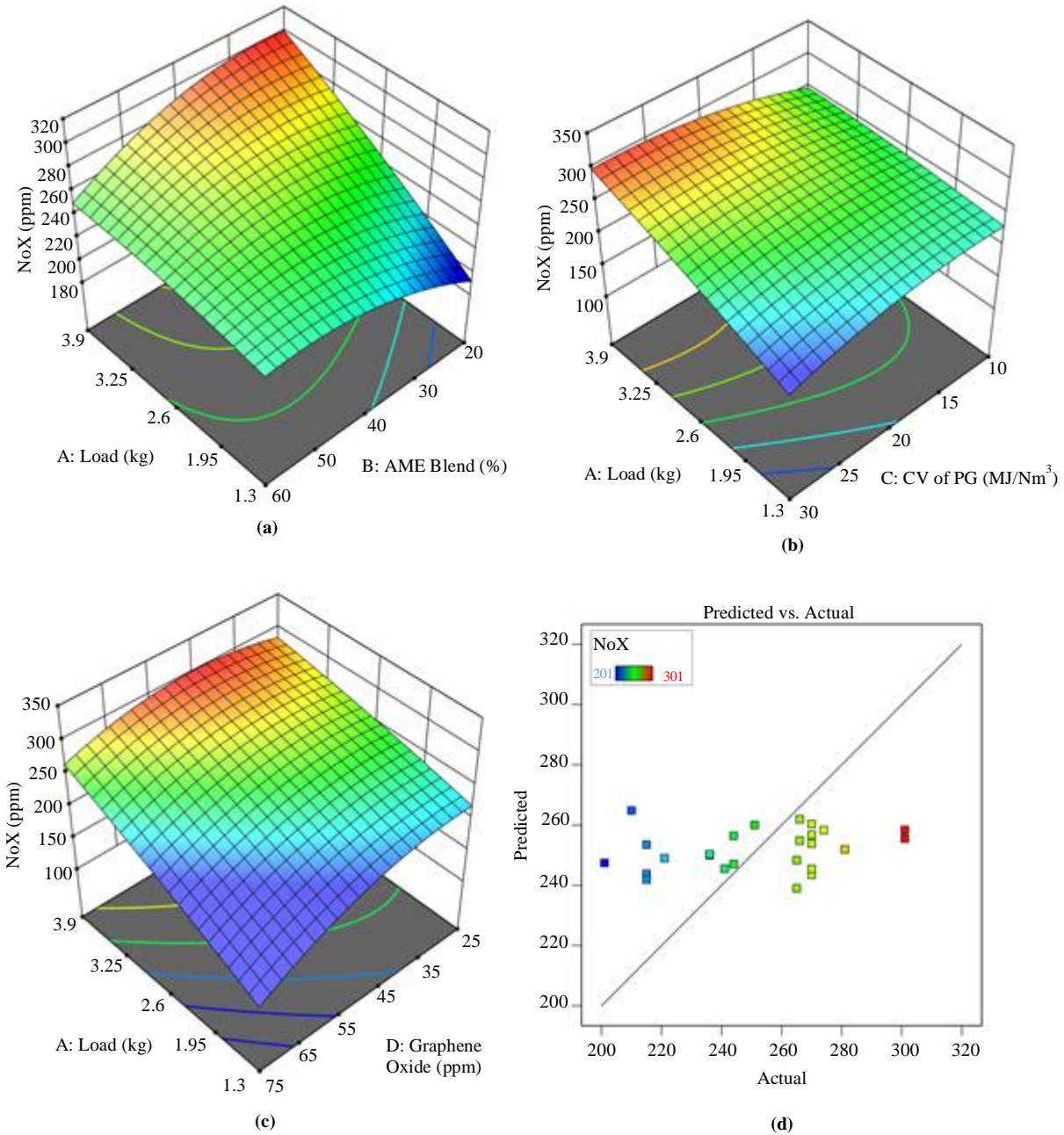


Fig. 7 NoX (a) Load vs. AME, (b) Load vs. CV of PG, (c) Load vs. Go, and (d) Predicated vs. Actual.

The exhaust smoke consists of solid carbon nanoparticles that are produced during combustion inside the fuel-rich portions of the cylinder, and it may be seen as exhaust smoke, which provides unwanted odorous pollution. The 3D surface plots shown in Figure 8(b) relate to the effect of the PG - CV and BP on the creation of exhaust smoke emissions. Smoke density, on the reverse together, rises in parallel with CV and BP. As CV decreases, PG velocity increases, reducing the rate

of airflow and resulting in insufficient air-fuel mixing. When low CV-producing gas is employed, this results in high smoke density. The 3D surface plots shown in Figure 8(c) related to the load vs Graphene Oxide; the surface graph shows an increase in smoke emission; Biodiesel and GO have been shown to be capable of reducing both smoke opacity and particle mass proportion of a diesel engine's exhaust gas. The amount of biodiesel and GO in the fuel reduces the opacity of

the smoke. The decrease in smoke opacity as biodiesel and GO levels increased could be related to a drop in carbon content as well as an increase in the amount of oxygen in the mixed fuel. Because the outcome falls within this range, the proposed

optimization's correctness is proven by the predicted and actual graphs shown in Figure 8(d). Lower emissions of smoke are reported at 21.01%, whereas more significant emissions of smoke are recorded at 35.4%.

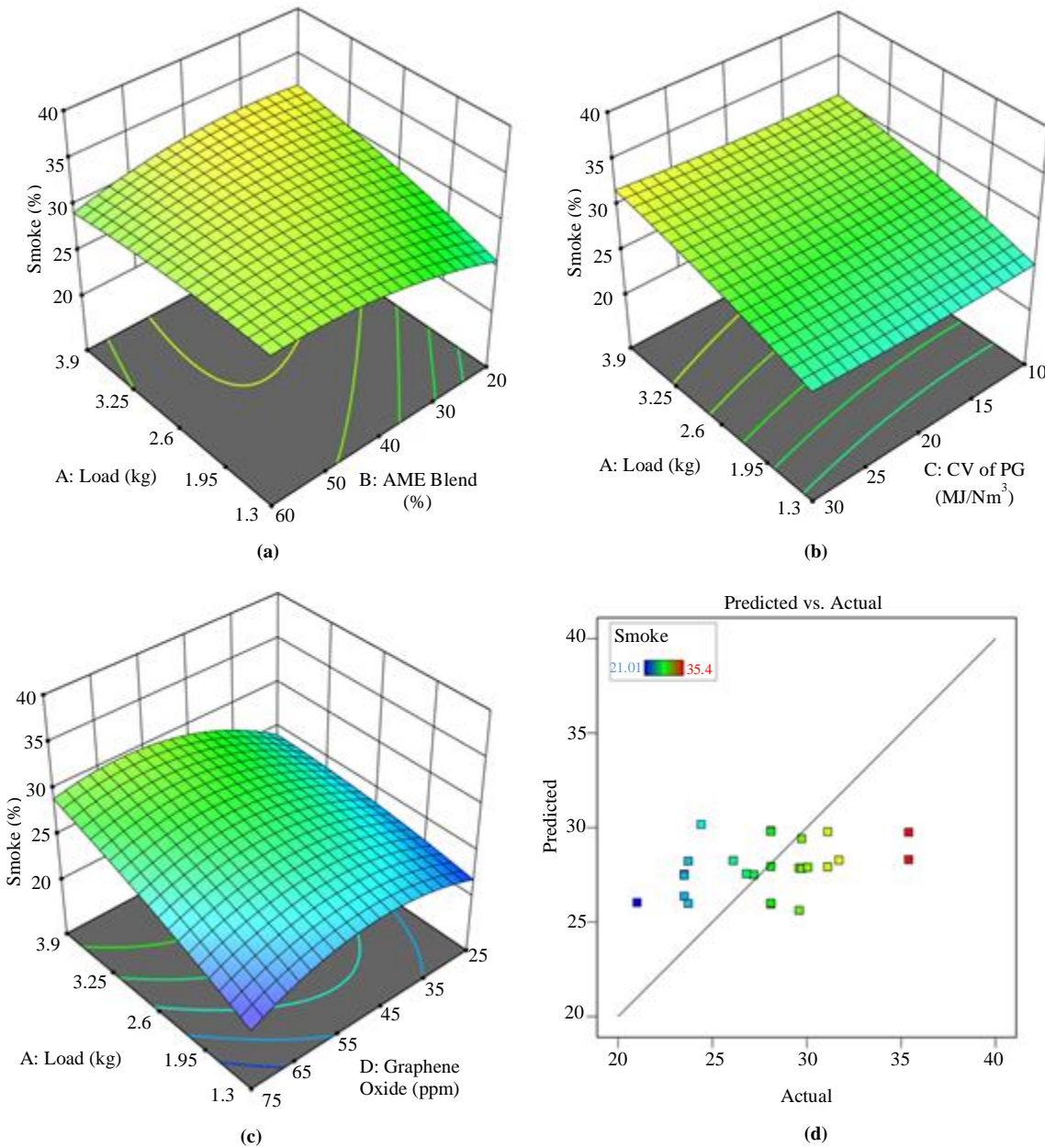


Fig 8. Smoke (a) Load vs. AME, (b) Load vs. CV of PG, (c) Load vs. Go, and (d) Predicated vs. Actual.

5. Conclusion

In an HCCI engine with a blend of 20, 40, and 60% algae methyl ester, this study investigated the effects of adding 25, 50, and 75 ppm Graphene Oxide(GO). It also included the CV of PG from 10, 20, and 30 MJ/Nm³ coconut shells with the smallest number of experiments necessary by optimising with RSM. Below is a summary of the results.

- BTE increases with an increase in BP and CV, which may be attributable to a high burn rate as well as rapid combustion progress. When low CV PG is delivered into the combustion area, it lowers the entering of fresh air, resulting in incomplete combustion and low BTE, where the lower BTE is 20.25% and the higher BTE is 26%.

- The decrease in BSFC with increasing BP could be attributed to the improved combustion characteristics of the PG/diesel mixture. Furthermore, greater combustion value and resultant decreases in fuel consumption happen due to increased fuel reaction provided by the additive, the lower BSFC being 1.69 kg/kWh and the higher BSFC being 2.46 kg/kWh.
- The change in CO emission, which constitutes one of the hazardous pollutants produced by partial combustion, relies on the GO and the load. Despite the reduction in CO emission caused by the addition of GO being nearly negligible, a modest decrease is observed in the lower CO content of the exhaust, which is 0.04 vol%, and the higher CO content is 0.22 vol%.
- HC emission reduces quickly with increasing GO quantity but increases quickly with increasing engine load. Because there is inadequate time for homogenous mixture production at high loads, the portion of the fuel will not meet with oxygen. HC is projected to rise as the load with the lower HC emission being 18.82 ppm and the higher HC emission being 30.3 ppm.
- The two main approaches for lowering NoX emissions, lowering the flame temperature and lowering the introduction of GO, promote a shorter combustion duration; the lower NoX emission is 201 ppm, whereas the more significant NoX emission is 301 ppm.
- The decrease in smoke opacity as biodiesel and GO levels increased could be related to a drop in carbon content as well as an increase in the amount of oxygen in the mixed fuel; lower smoke emissions are reported at 21.01%, whereas higher smoke emissions are reported at 35.4%.

5.1. Future Work

- Future studies can focus on the long-term effects of using graphene oxide dosed sesame oil/diesel fuel blend on engine durability and reliability.
- Further investigation on the influence of design parameters on performance and its relationship with calorific value and brake power.
- It would be beneficial to explore the potential of using other renewable fuels, such as biodiesel, in combination with Graphene Oxide to reduce harmful exhaust emissions further.
- Exploration of techniques using other renewable fuels to reduce CO and NoX emissions when using producer gas with higher calorific values.

Acknowledgments

The researchers thank the management of AVIT and the Vinayaka Mission Research Foundation for providing the laboratory resources.

References

- [1] Frederica Perera, "Pollution from Fossil-Fuel Combustion is the Leading Environmental Threat to Global Pediatric Health and Equity: Solutions Exist," *International Journal of Environmental Research and Public Health*, vol. 15, no. 1, pp. 1-17, 2018. [[CrossRef](#)] [[Google Scholar](#)] [[Publisher Link](#)]
- [2] Suleyman Simsek, Samet Uslu, and Hatice Simsek, "Response Surface Methodology-Based Parameter Optimization of Single-Cylinder Diesel Engine Fueled with Graphene Oxide Dosed Sesame Oil/Diesel Fuel Blend," *Energy and AI*, vol. 10, pp. 1-10, 2022. [[CrossRef](#)] [[Google Scholar](#)] [[Publisher Link](#)]
- [3] Golmohammad Khoobakht et al., "Optimization of Operating Factors and Blended Levels of Diesel, Biodiesel and Ethanol Fuels to Minimize Exhaust Emissions of Diesel Engine Using Response Surface Methodology," *Applied Thermal Engineering*, vol. 99, pp. 1006-1017, 2016. [[CrossRef](#)] [[Google Scholar](#)] [[Publisher Link](#)]
- [4] G. Arun Prasad et al., "Response Surface Methodology to Predict the Performance and Emission Characteristics of Gas-Diesel Engine Working on Producer Gases of Non-Uniform Calorific Values," *Energy*, vol. 234, 2021. [[CrossRef](#)] [[Google Scholar](#)] [[Publisher Link](#)]
- [5] Mathad R. Indudhar et al., "Optimization of Piston Grooves, Bridges on Cylinder Head, and Inlet Valve Masking of Home-Fueled Diesel Engine by Response Surface Methodology," *Sustainability*, vol. 13, no. 20, pp. 1-28, 2021. [[CrossRef](#)] [[Google Scholar](#)] [[Publisher Link](#)]
- [6] Hagar Alm ElDin Bastawissi et al., "Optimization of the Multi-Carburant Dose as an Energy Source for the Application of the HCCI Engine," *Fuel*, vol. 253, pp. 15-24, 2019. [[CrossRef](#)] [[Google Scholar](#)] [[Publisher Link](#)]
- [7] Harisankar Bendu, B.B.V.L. Deepak, and S. Murugan, "Multi-Objective Optimization of Ethanol Fuelled HCCI Engine Performance Using Hybrid GRNN-PSO," *Applied Energy*, vol. 187, pp. 601-611, 2017. [[CrossRef](#)] [[Google Scholar](#)] [[Publisher Link](#)]
- [8] Ganesh R. Gawale, and G. Naga Srinivasulu, "Experimental Investigation of Propanol Dual Fuel HCCI Engine Performance: Optimization of Propanol Mass Flow Rate, Impact of Butanol Blends (B10/B20/B30) as Fuel Substitute for Diesel," *Fuel*, vol. 279, 2020. [[CrossRef](#)] [[Google Scholar](#)] [[Publisher Link](#)]
- [9] Natarianto Indrawan et al., "Distributed Power Generation via Gasification of Biomass and Municipal Solid Waste: A Review," *Journal of the Energy Institute*, vol. 93, no. 6, pp. 2293-2313, 2020. [[CrossRef](#)] [[Google Scholar](#)] [[Publisher Link](#)]
- [10] Alpaslan Atmanli, Erol Ileri, and Nadir Yilmaz, "Optimization of Diesel-Butanol-Vegetable Oil Blend Ratios Based on Engine Operating Parameters," *Energy*, vol. 96, pp. 569-580, 2016. [[CrossRef](#)] [[Google Scholar](#)] [[Publisher Link](#)]

- [11] A.E. Dhole et al., "Mathematical Modeling for the Performance and Emission Parameters of Dual-Fuel Diesel Engine Using Producer Gas as Secondary Fuel," *Biomass Conversion and Biorefinery*, vol. 5, pp. 257-270, 2015. [[CrossRef](#)] [[Google Scholar](#)] [[Publisher Link](#)]
- [12] D.A. Baiseitov et al., "Research of the Combustion of Gas-Generating Compositions with Additives of Carbon Powders," *Materials Today: Proceedings*, vol. 33, no. 1, pp. 1216-1220, 2020. [[CrossRef](#)] [[Google Scholar](#)] [[Publisher Link](#)]
- [13] Cihan Bayindirli, Mehmet Celik, and Recep Zan, "Optimizing the Thermophysical Properties and Combustion Performance of Biodiesel by Graphite and Reduced Graphene Oxide Nanoparticle Fuel Additive," *Engineering Science and Technology, An International Journal*, vol. 37, pp. 1-12, 2023. [[CrossRef](#)] [[Google Scholar](#)] [[Publisher Link](#)]
- [14] Jiangjun Wei et al., "Comparison in the Effects of Alumina, Ceria and Silica Nanoparticle Additives on the Combustion and Emission Characteristics of A Modern Methanol-Diesel Dual-Fuel CI Engine," *Energy Conversion and Management*, vol. 238, 2021. [[CrossRef](#)] [[Google Scholar](#)] [[Publisher Link](#)]
- [15] Jong Boon Ooi et al., "Graphite Oxide Nanoparticle as A Diesel Fuel Additive for Cleaner Emissions and Lower Fuel Consumption," *Energy & Fuels*, vol. 30, no. 2, pp. 1341-1353, 2016. [[CrossRef](#)] [[Google Scholar](#)] [[Publisher Link](#)]
- [16] José Goldemberg, and Suani Teixeira Coelho, "Renewable Energy-Traditional Biomass vs. Modern Biomass," *Energy Policy*, vol. 32, no. 6, pp. 711-714, 2004. [[CrossRef](#)] [[Google Scholar](#)] [[Publisher Link](#)]
- [17] Yashvir Singh et al., "Optimization of Diesel Engine Performance and Emission Parameters Employing Cassia Tora Methyl Esters-Response Surface Methodology Approach," *Energy*, vol. 168, pp. 909-918, 2019. [[CrossRef](#)] [[Google Scholar](#)] [[Publisher Link](#)]
- [18] K. Prasada Rao, and B.V. Appa Rao, "Parametric Optimization for Performance and Emissions of An IDI Engine with Mahua Biodiesel," *Egyptian Journal of Petroleum*, vol. 26, no. 3, pp. 733-743, 2017. [[CrossRef](#)] [[Google Scholar](#)] [[Publisher Link](#)]
- [19] Adnan Berber, "Mathematical Model for Fuel Flow Performance of Diesel Engine," *International Journal of Automotive Engineering and Technologies*, vol. 5, no. 1, pp. 17-24, 2016. [[CrossRef](#)] [[Google Scholar](#)] [[Publisher Link](#)]
- [20] G. Najafi, "Diesel Engine Combustion Characteristics Using Nano-Particles in Biodiesel-Diesel Blends," *Fuel*, vol. 212, pp. 668-678, 2018. [[CrossRef](#)] [[Google Scholar](#)] [[Publisher Link](#)]
- [21] Mostafa Esmaili Shayan, Gholamhassan Najafi, and Giulio Lorenzini, "Optimization of A Dual Fuel Engine Based on Multi-Criteria Decision-Making Methods," *Thermal Science and Engineering Progress*, vol. 44, 2023. [[CrossRef](#)] [[Google Scholar](#)] [[Publisher Link](#)]
- [22] Shim Euijoon et al., "Comparisons of Advanced Combustion Technologies (HCCI, PCCI, and Dual-Fuel PCCI) on Engine Performance and Emission Characteristics in A Heavy-Duty Diesel Engine," *Fuel*, vol. 262, 2020. [[CrossRef](#)] [[Google Scholar](#)] [[Publisher Link](#)]
- [23] Ashish Nayyar et al., "Characterization of n-Butanol Diesel Blends on A Small Size Variable Compression Ratio Diesel Engine: Modeling and Experimental Investigation," *Energy Conversion and Management*, vol. 150, pp. 242-258, 2017. [[CrossRef](#)] [[Google Scholar](#)] [[Publisher Link](#)]
- [24] A. Pandal et al., "Optimization of Spray Break-Up CFD Simulations by Combining Σ -Y Eulerian Atomization Model with A Response Surface Methodology under Diesel Engine-Like Conditions (ECN Spray A)," *Computers & Fluids*, vol. 156, pp. 9-20, 2017. [[CrossRef](#)] [[Google Scholar](#)] [[Publisher Link](#)]
- [25] Takashi Kaminaga et al., "A Study on Combustion Characteristics of A High Compression Ratio SI Engine with High Pressure Gasoline Injection," *14th International Conference on Engines & Vehicles*, United States, pp. 1-22, 2019. [[CrossRef](#)] [[Google Scholar](#)] [[Publisher Link](#)]

Appendix

Table 3. Experimental design matrix for Algae Methyl Ester BLENDS, CV of PG and GO

Run	Load kg	AME Blend %	CV of PG MJ/Nm ³	Graphene Oxide ppm	BTE %	BSFC kg/kWh	CO vol%	HC ppm	NoX ppm	Smoke %
1	2.6	40	20	50	24.21	1.72	0.16	25.22	281	30.05
2	3.9	40	20	75	24.74	1.86	0.14	24.5	270	28.1
3	1.3	40	20	25	24.74	1.86	0.14	24.5	270	28.1
4	2.6	20	20	75	20.25	2.46	0.04	27.5	201	26.8
5	2.6	40	30	75	20.72	2.15	0.04	28.5	236	29.73
6	2.6	60	30	50	20.92	1.79	0.07	30.3	266	35.4
7	3.9	40	10	50	20.92	1.79	0.07	30.3	266	35.4
8	2.6	40	30	25	20.72	2.15	0.04	28.5	236	29.73
9	2.6	40	10	75	24.74	1.86	0.14	24.5	270	28.1
10	2.6	60	20	75	24.74	1.86	0.14	24.5	270	28.1
11	2.6	40	10	25	23.06	2.3	0.09	22.5	215	23.5
12	1.3	40	20	75	23.06	2.3	0.09	22.5	215	23.5
13	1.3	40	10	50	24.74	1.86	0.14	24.5	270	28.1
14	2.6	60	20	25	25.2	2.01	0.14	19.16	244	23.72
15	2.6	20	10	50	23.21	2.28	0.13	18.82	221	21.01
16	2.6	20	20	25	25.2	2.01	0.14	19.16	244	23.72
17	3.9	20	20	50	26	1.69	0.22	19.91	301	31.11
18	3.9	40	30	50	26	1.69	0.22	19.91	301	31.11
19	2.6	20	30	50	22.81	2.13	0.07	25.1	241	27.2
20	1.3	20	20	50	23.09	1.93	0.09	25.5	265	29.6
21	1.3	60	20	50	23.09	1.93	0.09	25.5	265	29.6
22	3.9	60	20	50	22.45	2.38	0.07	24.5	210	24.4
23	2.6	60	10	50	22.89	1.76	0.11	25.9	274	31.7
24	3.9	40	20	25	23.75	2.04	0.13	23.4	251	26.1
25	1.3	40	30	50	23.06	2.3	0.09	22.5	215	23.5

Table 4. Anova result

	A	B	C	D	AB	AC	AD	BC	BD	CD	A²	B²	C²	D²	R²
BTE	0.17	-0.11	-0.44	-0.37	-0.89	1.69	0.67	-0.39	1.12	-0.42	0.26	-0.46	-1.22	-0.33	0.76
p-values	0.74	0.84	0.41	0.49	0.34	0.09	0.47	0.67	0.24	0.65	0.81	0.67	0.28	0.76	
BSFC	-0.06	-0.06	0.03	0.01	0.17	-0.14	-0.16	0.05	-0.15	0.11	0.08	0.15	0.13	0.23	0.55
p-values	0.40	0.37	0.67	0.89	0.18	0.28	0.22	0.71	0.24	0.38	0.60	0.31	0.38	0.13	
CO	0.02	-0.01	-0.01	-0.01	-0.04	0.05	0.02	0.01	0.03	-0.01	0.00	-0.03	-0.04	-0.03	0.60
p-values	0.23	0.68	0.38	0.60	0.15	0.06	0.54	0.84	0.32	0.61	0.90	0.38	0.20	0.29	
HC	-0.21	1.16	0.69	1.23	1.15	-2.10	0.78	-0.47	-0.75	-0.50	-0.92	-1.13	0.81	-0.71	0.34
p-values	0.86	0.35	0.57	0.32	0.59	0.33	0.71	0.82	0.72	0.81	0.71	0.65	0.75	0.78	
NoX	8.25	4.67	-1.75	0.17	-22.7	22.50	18.50	-7.00	17.25	-13.75	-3.83	-15.96	-14.83	-25.96	0.61
p-values	0.31	0.56	0.82	0.98	0.12	0.12	0.20	0.61	0.22	0.33	0.81	0.34	0.37	0.13	
Smoke	1.15	1.12	0.74	0.79	-1.68	0.08	1.65	-0.62	0.33	-1.15	-0.50	-1.29	0.23	-2.93	0.38
p-values	0.39	0.40	0.58	0.55	0.47	0.97	0.48	0.79	0.89	0.62	0.85	0.64	0.93	0.30	